Mineralogical Magazine, April 2015, Vol. 79(2), pp. 345–354

Tapiaite, $Ca_5Al_2(AsO_4)_4(OH)_4 \cdot 12H_2O$, a new mineral from the Jote mine, Tierra Amarilla, Chile

ANTHONY R. KAMPF[1,*], STUART J. MILLS[2], BARBARA P. NASH[3], MAURIZIO DINI[4] AND ARTURO A. MOLINA DONOSO[5]

[1] Mineral Sciences Department, Natural History Museum of Los Angeles County, 900 Exposition Boulevard, Los Angeles, CA 90007, USA
[2] Geosciences, Museum Victoria, GPO Box 666, Melbourne 3001, Victoria, Australia
[3] Department of Geology and Geophysics, University of Utah, Salt Lake City, Utah 84112, USA
[4] Pasaje San Agustin 4045, La Serena, Chile
[5] Los Algarrobos 2986, Iquique, Chile

[*Received 22 June 2014; Accepted 20 August 2014; Associate Editor: I. Graham*]

ABSTRACT

Tapiaite (IMA2014-024), $Ca_5Al_2(AsO_4)_4(OH)_4 \cdot 12H_2O$, is a new mineral from the Jote mine, Tierra Amarilla, Copiapó Province, Atacama, Chile. The mineral is a late-stage, low-temperature, secondary mineral occurring with conichalcite, joteite, mansfieldite, pharmacoalumite, pharmacosiderite and scorodite in narrow seams and vughs in the oxidized upper portion of a hydrothermal sulfide vein hosted by volcanoclastic rocks. Crystals occur as colourless blades, flattened on $\{10\bar{1}\}$ and elongated and striated along [010], up to ~0.5 mm long, and exhibiting the forms $\{10\bar{1}\}$, $\{101\}$ and $\{111\}$. The blades are commonly intergrown in subparallel bundles and less commonly in sprays. The mineral is transparent and has a white streak and vitreous lustre. The Mohs hardness is estimated to be between 2 and 3, the tenacity is brittle, and the fracture is splintery. It has two perfect cleavages on $\{101\}$ and $\{10\bar{1}\}$. The calculated density based on the empirical formula is 2.681 g cm^{-3}. It is optically biaxial (+) with α = 1.579(1), β = 1.588(1), γ = 1.610(1) (white light), $2V_{meas}$ = 66(2)º and $2V_{calc}$ = 66º. The mineral exhibits no dispersion. The optical orientation is $X \approx [10\bar{1}]$; $Y = b$, $Z \approx [101]$. The electron-microprobe analyses (average of five) provided: Na_2O 0.09, CaO 24.96, CuO 0.73, Al_2O_3 10.08, Fe_2O_3 0.19, As_2O_5 40.98, Sb_2O_5 0.09, H_2O 23.46 (structure), total 100.58 wt.%. In terms of the structure, the empirical formula (based on 32 O a.p.f.u.) is $(Ca_{4.83}Cu^{2+}_{0.10}Na_{0.03})_{\Sigma 4.96}(Al_{2.14}Fe^{3+}_{0.03})_{\Sigma 2.17}[(As^{5+}_{3.87}Sb^{5+}_{0.01})_{\Sigma 3.88}O_{16}][(OH)_{3.76}(H_2O)_{0.24}]_{\Sigma 4}(H_2O)_{10} \cdot 2H_2O$. The mineral is easily soluble in RT dilute HCl. Tapiaite is monoclinic, $P2_1/n$, with unit-cell parameters a = 16.016(1), b = 5.7781(3), c = 16.341(1) Å, β = 116.704(8)º, V = 1350.9(2) Å^3 and Z = 2. The eight strongest lines in the powder X-ray diffraction pattern are [d_{obs} Å(I)(hkl)]: 13.91(100)($\bar{1}01$), 7.23(17)(200,002), 5.39(22)(110,011), 4.64(33)($\bar{1}12,\bar{2}11,\bar{3}03$), 3.952(42)($\bar{1}13,\bar{3}11,\bar{2}13$), 3.290(35)($\bar{2}14,\bar{4}12,\bar{1}14,\bar{4}11$), 2.823(39)(303,$\bar{3}15$) and 2.753(15)($\bar{5}13,\bar{1}15,121,\bar{5}11$). The structure of tapiaite (R_1 = 5.37% for 1733 $F_o > 4\sigma F$) contains $Al(AsO_4)(OH)_2$ chains of octahedra and tetrahedra that are topologically identical to the chain in the structure of linarite. CaO_8 polyhedra condense to the chains, forming columns, which are decorated with additional peripheral AsO_4 tetrahedra. The CaO_8 polyhedra in adjacent columns link to one another by corner-sharing to form thick layers parallel to $\{10\bar{1}\}$ and the peripheral AsO_4 tetrahedra link to CaO_6 octahedra in the interlayer region, resulting in a framework structure.

KEYWORDS: tapiaite, new mineral, arsenate, crystal structure, Jote mine, Tierra Amarilla, Chile.

* E-mail: akampf@nhm.org
DOI: 10.1180/minmag.2015.079.2.12

Introduction

Renewed interest in the mineralogy of the small mines and prospects of the Pampa Larga mining district, Atacama Region, Chile, has resulted in the discovery of several new and/or rare secondary As minerals. Efforts by the present authors have focused on the small Jote mine, where in 2007 Robert A. Jenkins collected the first specimens of the new mineral joteite, $Ca_2CuAl[AsO_4][AsO_3(OH)]_2(OH)_2{\cdot}5H_2O$ (Kampf *et al*., 2013). Subsequent visits by one of the authors (AAMD) in 2011 and 2012 yielded additional specimens of joteite, as well as several other potentially new minerals. One new mineral, which occurs intimately associated with joteite, is the subject of this paper.

The new mineral is named tapiaite /ˈtɑ pi: ə aɪt/ for Enrique Tapia (1955–2008), a well known Chilean mineral collector. Enrique was one of the first and most influential individuals to promote mineral collecting in northern Chile and the Atacama Desert, in particular. He collected in several areas of the Atacama, including the mines of the Pampa Larga district (Veta Negra, Alacrán, Descubridora and Jote). He was distinguished for his untiring collecting spirit. He died unexpectedly of leukemia in March 2008, while preparing to leave on a collecting excursion.

The new mineral and name have been approved by the Commission on New Minerals, Nomenclature and Classification of the International Mineralogical Association (IMA2014-024, Kampf *et al*., 2014). The description of the new mineral was based upon four specimens, which are designated cotype specimens and are deposited in the Natural History Museum of Los Angeles County, under catalogue numbers 63594, 64123, 64124 and 64125. Specimen 63594 is also a cotype for joteite.

Occurrence and paragenesis

The mineral occurs at the Jote mine, Pampa Larga district, Tierra Amarilla, Copiapó Province, Atacama Region, Chile. Mineralization occurs in a narrow (20–40 cm wide) hydrothermal vein hosted by volcanoclastic rocks. The occurrence is similar to that of rruffite (Yang *et al*., 2011) at the Maria Catalina mine in the same district. A detailed description of the geology and mineralogy of the area was provided by Parker *et al*. (1963). The specimens of tapiaite were collected by one of the authors (AAMD) in 2011.

The deeper unoxidized portion of the vein contains primary and supergene minerals including acanthite, native arsenic, Ag sulfosalts, baryte, calcite, chalcopyrite, domeykite, feldspar, pyrite, quartz, native silver and stibnite. Tapiaite occurs as a late-stage, low-temperature, secondary mineral in narrow seams and vughs in the oxidized upper portion of the vein. The matrix is an intergrowth of quartz and microcline–albite 'microperthite'. The microperthite varies from fresh to heavily altered. The more heavily altered areas are impregnated with massive mansfieldite and/or scorodite. Other secondary minerals in direct association with tapiaite are conichalcite, joteite, pharmacoalumite and pharmacosiderite. Other minerals found in the oxidation zone include arseniosiderite, ceruleite, chlorargyrite, gartrellite, goudeyite, gypsum, karibibite, koritnigite, krautite, lavendulan, lotharmeyerite, metazeunerite, olivenite, opal, rruffite, siderite and zincolivenite. In addition, we confirmed remnants of domeykite, Cu_3As, as brassy iridescent patches embedded in lavendulan in the oxidation zone. We consider this to be of particular significance, both because of the rarity of the species and because of its possible genetic relation to the rare secondary arsenate species found at this and other deposits in the area.

Physical and optical properties

Crystals occur as blades up to ~0.5 mm × 0.05 mm × 0.01 mm in size, but are usually much smaller. The blades are commonly intergrown in sub-parallel bundles and less commonly in sprays (Fig. 1). The blades are flattened on $\{10\bar{1}\}$,

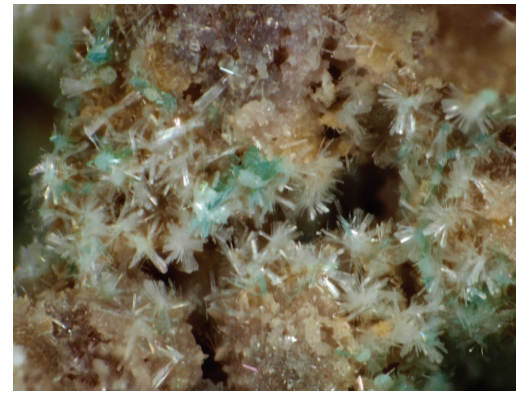

Fig. 1. Colourless tapiaite blades with blue-green joteite (Field of view: 2 mm).

elongated and striated along [010] and exhibit the forms $\{10\bar{1}\}$, $\{101\}$ and $\{111\}$ (Fig. 2). No twinning was observed. Tapiaite is colourless and has a white streak. Crystals are transparent and have vitreous lustre. Tapiaite does not fluoresce in longwave or shortwave ultraviolet light. The Mohs hardness is estimated to be between 2 and 3. The tenacity is brittle and the fracture is splintery. Crystals exhibit perfect cleavage on $\{101\}$ and $\{10\bar{1}\}$. Attempts to measure the density by sink-float in Clerici solution were unsuccessful because the crystals proved too difficult to see. The calculated density is 2.681 g cm^{-3} based on the empirical formula and 2.690 g cm^{-3} based on the ideal formula. Tapiaite is easily soluble in room-temperature dilute HCl and slowly soluble in H_2O.

Optically, tapiaite is biaxial (+), with α = 1.579(1), β = 1.588(1) and γ = 1.610(1), measured in white light. The 2V measured directly by conoscopic observation is 66(2)º. The calculated 2V is 66.0º. The mineral exhibits no perceptible dispersion. The optical orientation is $X \approx [10\bar{1}]$; $Y = b$, $Z \approx [101]$. Tapiaite is non-pleochroic.

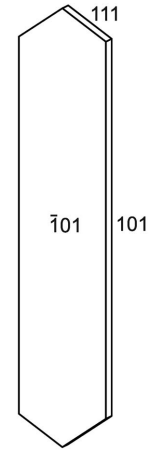

FIG. 2. Crystal drawing of tapiaite (clinographic projection in non-standard orientation).

Chemical composition

Five chemical analyses, each on a separate crystal, were carried out at the University of Utah on a Cameca SX-50 electron microprobe with four wavelength dispersive spectrometers. Analytical conditions were 15 kV accelerating voltage, 20 nA beam current and a beam diameter of 10 μm. Counting times were 10 s on peak and background for each element. Additional elements sought that were below the limits of detection include Mg, K, Mn and Co. Raw X-ray intensities were corrected for matrix effects with a $\phi(\rho z)$ algorithm (Pouchou and Pichoir, 1991). Sodium, As and Sb were analysed first on the spectrometers. Minor Na migration under the beam was observed, so a time-dependent correction for the Na intensities was employed. The associated species suggest that all Fe in tapiaite is Fe^{3+}. Crystals exhibited moderate beam damage.

Because insufficient material was available for a direct determination of H_2O, the amount of water in tapiaite was calculated on the basis of 11 total cations (Ca+Na+Cu+Al+Fe+As+Sb), charge balance and 32 O atoms per formula unit (a.p.f.u.), as determined by the crystal structure analysis (see below). Analytical data and standards are given in Table 1.

TABLE 1. Analytical data for tapiaite.

Constituent	Wt.%	Range	SD	Standard
Na_2O	0.09	0.04–0.16	0.05	Albite
CaO	24.96	24.13–25.89	0.70	Diopside
CuO	0.73	0.15–1.75	0.72	Cu metal
Al_2O_3	10.08	9.48–10.70	0.47	Syn. YAG
Fe_2O_3	0.19	0.04–0.41	0.14	Hematite
As_2O_5	40.98	39.84–42.56	1.03	Syn. GaAs
Sb_2O_5	0.09	0.07–0.13	0.02	Syn. GaSb
H_2O*	23.46			
Total	100.58			

* Calculated based on the structure.

The empirical formula (based on O = 32 a.p.f.u.) is $Na_{0.03}Ca_{4.83}Cu^{2+}_{0.10}Al_{2.14}Fe^{3+}_{0.03}As^{5+}_{3.87}Sb^{5+}_{0.01}O_{32}H_{28.24}$. The simplified formula is $Ca_5Al_2(AsO_4)_4(OH)_4{\cdot}12H_2O$, which requires CaO 25.62, Al_2O_3 9.32, As_2O_5 42.01, H_2O 23.05, total 100 wt.%. The Gladstone-Dale compatibility index $1 - (K_P/K_C)$ is −0.003 for the empirical formula, indicating superior compatibility (Mandarino, 2007).

The structural formula may be written $Ca_5Al_2(AsO_4)_4(OH)_4(H_2O)_{10}{\cdot}2H_2O$, indicating that one H_2O group (OW16) does not bond to

TABLE 2. Powder X-ray data for tapiaite.

I_{obs}	d_{obs}	d_{calc}	I_{calc}	*h k l*
100	13.91	13.7693	100	$\bar{1}$ 0 1
12	8.55	8.4878	12	1 0 1
17	7.23	7.2990	9	0 0 2
		7.1539	10	2 0 0
		6.8847	4	$\bar{2}$ 0 2
22	5.39	5.3726	5	0 1 1
		5.3577	5	1 1 0
33	4.64	4.7140	4	$\bar{1}$ 1 2
		4.6840	3	$\bar{2}$ 1 1
		4.5898	6	$\bar{3}$ 0 3
42	3.952	4.0302	3	3 0 1
		3.9999	2	$\bar{4}$ 0 2
		3.9907	1	2 1 1
		3.9479	6	$\bar{1}$ 1 3
		3.9014	5	$\bar{3}$ 1 1
		3.8953	6	$\bar{2}$ 1 3
		3.8671	5	$\bar{3}$ 1 2
3	3.441	3.4423	3	$\bar{4}$ 0 4
35	3.290	3.3306	7	$\bar{2}$ 1 4
		3.2887	6	$\bar{4}$ 1 2
		3.2843	9	$\bar{1}$ 1 4
		3.2344	8	$\bar{4}$ 1 1
		3.1515	3	$\bar{1}$ 0 5
12	3.084	3.0856	5	0 1 4
		3.0817	3	$\bar{5}$ 0 1
		3.0413	5	4 1 0
		2.9049	3	3 1 2
39	2.823	2.8293	15	3 0 3
		2.8096	6	$\bar{3}$ 1 5
15	2.753	2.7760	7	$\bar{5}$ 1 3
		2.7667	4	$\bar{1}$ 1 5
		2.7350	7	1 2 1
		2.7191	4	$\bar{5}$ 1 1
5	2.657	2.6640	2	$\bar{2}$ 2 2
		2.6445	1	$\bar{6}$ 0 2
		2.6379	2	1 0 5
3	2.611	2.6058	2	0 1 5
		2.5965	2	5 0 1
2	2.506	2.5079	1	2 1 4
		2.4899	2	4 1 2
10	2.343	2.3570	2	$\bar{2}$ 2 4
		2.3420	2	$\bar{4}$ 2 2
		2.3404	2	$\bar{1}$ 2 4
		2.3342	2	$\bar{3}$ 0 7
4	2.301	2.2949	3	$\bar{6}$ 0 6
		2.2868	2	$\bar{7}$ 0 3
5	2.214	2.2130	4	$\bar{4}$ 2 4
9	2.137	2.1360	1	$\bar{2}$ 1 7
		2.1339	1	$\bar{5}$ 2 3
		2.1326	1	4 2 1
		2.1263	1	$\bar{7}$ 1 3
12	2.0000	2.0046	3	2 2 4
		1.9954	3	4 2 2
		1.9934	1	$\bar{5}$ 2 5
		1.9919	1	4 1 4
15	1.8070	1.8133	2	7 1 1
		1.8092	2	$\bar{2}$ 3 3
		1.8063	1	$\bar{3}$ 3 2
		1.8022	2	$\bar{3}$ 0 9
		1.7909	2	0 3 3
12	1.7555	1.7643	2	$\bar{5}$ 2 7
		1.7630	3	$\bar{9}$ 0 3
		1.7539	1	2 3 2
		1.7518	2	$\bar{7}$ 2 5
		1.7401	2	0 1 8
7	1.7117	1.7212	1	$\bar{8}$ 0 8
		1.7158	1	2 1 7
		1.7102	2	4 2 4
		1.7085	2	8 1 0
		1.6653	3	$\bar{4}$ 2 8
12	1.6493	1.6523	1	$\bar{3}$ 3 5
		1.6508	1	$\bar{9}$ 1 2
		1.6444	3	$\bar{8}$ 2 4
		1.6434	1	$\bar{1}$ 3 5
		1.6422	1	$\bar{2}$ 2 8
6	1.6142	1.6186	1	8 1 1
		1.6172	1	$\bar{8}$ 2 2
		1.6122	1	1 2 7
6	1.5991	1.6077	2	0 3 5
		1.6039	1	2 0 8
		1.6024	1	$\bar{6}$ 2 8
		1.5978	1	5 3 0
		1.5932	2	7 2 1
		1.5915	1	$\bar{8}$ 2 6
5	1.5463	1.5563	1	$\bar{8}$ 1 9
		1.5502	1	$\bar{9}$ 1 8
		1.5455	1	2 1 8
		1.5428	1	0 2 8

Only calculated lines with intensities >3 are listed unless they correspond to observed lines.

any cation. A deficiency of 3% in pentavalent cations (As + Sb) in the empirical formula may be real, as the structure refinement also indicates 3% less than full occupancy in the *As* sites. It seems most likely that the 0.03 Na and 0.10 Cu^{2+} a.p.f.u. in the empirical formula are accommodated in the *Ca*1 site; however, there appears to be no way to accommodate the 0.17 a.p.f.u. surplus of trivalent cations (Al + Fe) in the structure. Therefore, this surplus is attributed to experimental error, possibly related to sample instability in the beam and/or heterogeneity of the crystals. In terms of the structure, the empirical formula can be written $(Ca_{4.83}Cu^{2+}_{0.10}Na_{0.03})_{\Sigma 4.96}(Al_{2.14}Fe^{3+}_{0.03})_{\Sigma 2.17}[(As^{5+}_{3.87}Sb^{5+}_{0.01})_{\Sigma 3.88}O_{16}][(OH)_{3.76}(H_2O)_{0.24}]_{\Sigma 4}(H_2O)_{10}\cdot 2H_2O$.

X-ray crystallography and structure refinement

Both powder and single-crystal X-ray studies were carried out using a Rigaku R-Axis Rapid II curved imaging plate microdiffractometer, with monochromatized Mo$K\alpha$ radiation. For the powder-diffraction study, a Gandolfi-like motion on the φ and ω axes was used to randomize the sample and observed *d*-spacings and intensities were derived by profile fitting using *JADE 2010* software (Materials Data, Inc.). The powder data presented in Table 2 show good agreement with the pattern calculated from the structure determination. Unit-cell parameters refined from the powder data using *JADE 2010* with whole-pattern fitting are: a = 16.008(8), b = 5.767(9), c = 16.367(8) Å, β = 116.72(2)º and V = 1350 (2) Å^3.

In the single-crystal study, a total of 48 frames at 50-min exposures were recorded. The Rigaku *CrystalClear* software package was used for processing the structure data, including the application of an empirical multi-scan absorption correction using *ABSCOR* (Higashi, 2001). The structure was solved by direct methods using *SHELXS* and was refined using *SHELXL* (Sheldrick, 2008). Site-occupancy refinements

TABLE 3. Data-collection and structure-refinement details for tapiaite.

Diffractometer	Rigaku R-Axis Rapid II
X-ray radiation/power	Mo$K\alpha$ (λ = 0.71075 Å)/50 kV, 40 mA
Temperature	298(2) K
Ideal structural formula	$Ca_5Al_2(AsO_4)_4(OH)_4(H_2O)_{10}\cdot 2H_2O$
Space group	$P2_1/n$
Unit-cell dimensions	a = 16.0160(12) Å
	b = 5.7781(3) Å
	c = 16.3410(12) Å
	β = 116.704(8)º
V	1350.93(16) Å^3
Z	2
Density (for above formula)	2.690 g cm^{-3}
Abs. coefficient (for above formula)	6.047 mm^{-1}
F(000)	1084
Crystal size	70 μm × 30 μm × 10 μm
θ range	3.77–25.02º
Index ranges	$-19 \leqslant h \leqslant 19$, $-6 \leqslant k \leqslant 6$, $-19 \leqslant l \leqslant 19$
Reflections collected/unique	10,063 / 2357 [R_{int} = 0.087]
Reflections with $F_o > 4\sigma(F)$	1733
Completeness to θ = 25.02º	98.7%
Max. and min. transmission	0.942 and 0.677
Refinement method	Full-matrix least-squares on F^2
Parameters refined	198
Gof	1.047
Final R indices [$F_o > 4\sigma(F)$]	R_1 = 0.0537, wR_2 = 0.1253
R indices (all data)	R_1 = 0.0784, wR_2 = 0.1420
Largest diff. peak / hole	+2.05 / −0.84 e A^{-3}

$R_{int} = \Sigma|F_o^2 - F_o^2(\text{mean})|/\Sigma[F_o^2]$. Gof = $S = \{\Sigma[w(F_o^2-F_c^2)^2]/(n-p)\}^{1/2}$. $R_1 = \Sigma||F_o|-|F_c||/\Sigma|F_o|$. $wR_2 = \{\Sigma[w(F_o^2-F_c^2)^2]/\Sigma[w(F_o^2)^2]\}^{1/2}$. $w = 1/[\sigma^2(F_o^2)+(aP)^2 + bP]$ where a is 0.0789, b is 0.4203 and P is $[2F_c^2+\text{Max}(F_o^2,0)]/3$.

TABLE 4. Atom coordinates and displacement parameters (Å^2) for tapiaite.

	x/*a*	*y*/*b*	*z*/*c*	U_{eq}	U^{11}	U^{22}	U^{33}	U^{23}	U^{13}	U^{12}
Ca1	½	½	0	0.0209(6)	0.0262(14)	0.0181(12)	0.0232(15)	0.0017(10)	0.0154(12)	0.0017(9)
Ca2	0.47839(11)	0.1855(3)	0.33149(12)	0.0187(5)	0.0196(9)	0.0185(9)	0.0163(10)	−0.0012(7)	0.0066(8)	−0.0022(6)
Ca3	0.32828(11)	0.3149(3)	0.47120(12)	0.0188(5)	0.0165(9)	0.0199(9)	0.0195(10)	0.0026(7)	0.0076(8)	0.0003(7)
Al	0.74473(16)	0.4993(3)	0.75492(16)	0.0131(6)	0.0156(13)	0.0097(11)	0.0135(14)	−0.0007(9)	0.0059(11)	0.0003(8)
As1*	0.57805(6)	0.24950(12)	0.57888(6)	0.0135(3)	0.0135(5)	0.0114(5)	0.0134(5)	0.0003(3)	0.0039(4)	−0.0006(3)
As2*	0.41220(6)	0.99716(13)	0.09523(6)	0.0149(3)	0.0169(5)	0.0130(5)	0.0171(5)	−0.0001(3)	0.0098(4)	0.0002(3)
O1	0.4764(4)	0.1762(9)	0.5750(4)	0.0188(13)	0.016(3)	0.017(3)	0.027(4)	0.001(2)	0.012(3)	−0.001(2)
O2	0.5762(4)	0.3224(9)	0.4798(4)	0.0199(13)	0.028(3)	0.021(3)	0.013(3)	0.004(2)	0.012(3)	0.006(2)
O3	0.6282(4)	0.4860(8)	0.6444(4)	0.0168(12)	0.017(3)	0.012(3)	0.017(3)	0.006(2)	0.004(3)	0.005(2)
O4	0.6446(4)	0.0114(8)	0.6299(4)	0.0161(12)	0.018(3)	0.013(3)	0.017(3)	−0.005(2)	0.009(3)	−0.003(2)
O5	0.4156(4)	0.7683(9)	0.0344(4)	0.0261(15)	0.030(4)	0.020(3)	0.034(4)	−0.008(2)	0.020(3)	0.003(2)
O6	0.4776(4)	0.2168(9)	0.0892(4)	0.0267(14)	0.030(4)	0.025(3)	0.031(4)	0.002(3)	0.019(3)	−0.006(2)
O7	0.2998(4)	0.0821(8)	0.0575(4)	0.0218(13)	0.024(3)	0.013(3)	0.028(4)	−0.001(2)	0.012(3)	−0.003(2)
O8	0.4500(4)	0.9225(8)	0.2067(4)	0.0186(13)	0.022(3)	0.014(3)	0.018(3)	0.000(2)	0.008(3)	−0.001(2)
OH9	0.3045(4)	0.2357(8)	0.2162(4)	0.0186(13)	0.020(3)	0.018(3)	0.018(3)	0.000(2)	0.008(3)	0.002(2)
OH10	0.2139(4)	0.2656(8)	0.3027(4)	0.0158(12)	0.016(3)	0.019(3)	0.011(3)	−0.003(2)	0.004(3)	−0.002(2)
OW11	0.4958(5)	0.4791(9)	0.2378(4)	0.0302(15)	0.042(4)	0.024(3)	0.030(4)	0.006(3)	0.020(3)	0.004(3)
OW12	0.6357(4)	0.1245(10)	0.3388(5)	0.0332(16)	0.031(4)	0.031(4)	0.033(4)	0.004(3)	0.010(3)	0.006(3)
OW13	0.6394(5)	0.5986(11)	0.1367(5)	0.0423(18)	0.041(4)	0.040(4)	0.036(5)	−0.001(3)	0.009(4)	−0.004(3)
OW14	0.2365(4)	0.0218(9)	0.4928(5)	0.0263(15)	0.024(3)	0.018(3)	0.038(4)	0.000(3)	0.016(3)	−0.007(2)
OW15	0.6780(5)	0.6029(10)	0.3769(5)	0.0365(17)	0.048(4)	0.034(4)	0.033(4)	−0.008(3)	0.024(4)	−0.011(3)
OW16	0.8347(5)	0.5687(12)	0.3282(5)	0.0455(19)	0.045(5)	0.042(4)	0.040(5)	−0.002(3)	0.011(4)	−0.006(3)

* Refined occupancies: As1 = 0.967(5); As2 = 0.972(5).

were attempted for each site. All sites refined to very close to full occupancy, except the *As*1 and *As*2 sites, which refined to 0.967(5) and 0.972(5), respectively. This matches closely the 3% deficiency in As + Sb in the empirical formula. As mentioned above, the 0.03 Na and 0.10 Cu^{2+} a.p.f.u. in the empirical formula are probably accommodated in the *Ca*1 site. The full occupancy of this site, indicated by the structure refinement, is consistent with this interpretation, considering that Na and Cu would have offsetting effects on the site scattering and there may be a small vacancy at the site.

Data collection and structure refinement details are provided in Table 3, atom coordinates and displacement parameters in Table 4, selected bond distances in Table 5 and bond-valence summations in Table 6. Lists of observed and calculated structure factors have been deposited with the Principal Editor of *Mineralogical Magazine* and are available from www.minersoc.org/pages/e_journals/dep_mat_mm.html.

Description of the structure

The structure of tapiaite is shown in Fig. 3. The backbone of the structure is a chain of *trans*-edge-sharing AlO_6 octahedra. The remaining vertices of adjacent octahedra are further linked to one another by AsO_4 tetrahedra (As1), in a staggered arrangement, forming $Al(AsO_4)(OH)_2$ chains of octahedra and tetrahedra (Fig. 4) parallel to the *b* axis. The chain of octahedra and tetrahedra is topologically identical to that in the structure of linarite, $PbCu(SO_4)(OH)_2$ (Schofield *et al*., 2009). Similar chains, but decorated with additional tetrahedra, are found in the structures of brackebuschite group and related minerals (Huminicki and Hawthorne 2002), e.g. bearthite, $Ca_2Al(PO_4)_2(OH)$ (Chopin *et al*., 1993) and vauquelinite, $Pb_2Cu(CrO_4)(PO_4)(OH)$ (Fanfani and Zanazzi, 1968). Similar chains, but with addenda tetrahedra and octahedra, are found in the structures of kapundaite, $(Na,Ca)_2Fe_4^{3+}(PO_4)_4(OH)_3{\cdot}5H_2O$ (Mills *et al*., 2010) and mélonjosephite, $CaFe^{2+}Fe^{3+}(PO_4)_2(OH)$ (Kampf and Moore, 1977).

CaO_8 polyhedra (Ca2 and Ca3) condense to the chain by edge- and corner-sharing with the octahedra and tetrahedra in the chain, thereby forming broad chains or columns. The CaO_8 polyhedra in adjacent columns link to one another by corner-sharing to form thick layers parallel to $\{10\bar{1}\}$. Additional AsO_4 tetrahedra (As2) decorate

TABLE 5. Selected bond distances (Å) in tapiaite.

Ca1–O5 (×2)	2.286(5)	Ca2–O2	2.354(6)	Ca3–O1	2.351(6)			
Ca1–O6 (×2)	2.324(6)	Ca2–OW11	2.383(6)	Ca3–OW14	2.370(6)	Hydrogen bonds		
Ca1–OW13 (×2)	2.412(7)	Ca2–O8	2.417(6)	Ca3–O7	2.439(5)	OH9–O7	2.711(8)	
<Ca1–O>	2.341	Ca2–OW12	2.493(6)	Ca3–O2	2.504(6)	OH10–O8	2.715(7)	
		Ca2–O1	2.497(5)	Ca3–OH10	2.547(6)	OW11–O8	2.651(7)	
Al–OH9	1.877(5)	Ca2–OH9	2.584(6)	Ca3–O3	2.561(5)	OW11–O6	2.765(9)	
Al–OH10	1.882(5)	Ca2–O4	2.586(5)	Ca3–OW15	2.573(7)	OW12–OW14	2.723(9)	
Al–O4	1.921(6)	Ca2–O3	2.698(5)	Ca3–O4	2.669(5)	OW12–OW15	2.847(8)	
Al–OH9	1.925(6)	<Ca2–O>	2.502	<Ca3–O>	2.502	OW13–OW16	2.769(9)	
Al–O3	1.929(6)					OW13–OW16	3.108(9)	
Al–OH10	1.932(6)	As1–O1	1.656(5)	As2–O5	1.670(5)	OW14–O7	2.653(7)	
<Al–O>	1.911	As1–O2	1.661(5)	As2–O6	1.677(5)	OW14–O5	2.682(8)	
		As1–O3	1.699(5)	As2–O7	1.692(5)	OW15–OW11	2.869(9)	
		As1–O4	1.710(5)	As2–O8	1.697(6)	OW15–OW16	2.960(10)	
		<As1–O>	1.682	<As2–O>	1.685	OW16–O6	2.819(9)	
						OW16–OW12	2.990(10)	

TABLE 6. Bond-valence analysis for tapiaite. Values are expressed in valence units.

	O1	O2	O3	O4	O5	O6	O7	O8	OH9	OH10	OW11	OW12	OW13	OH14	OW15	OW16	Σ_c
Ca1					$0.42^{\times 2\rightarrow}$	$0.38^{\times 2\rightarrow}$							$0.30^{\times 2\rightarrow}$				2.20
Ca2	0.24	0.35	0.14	0.19				0.30	0.19		0.32	0.24					1.97
Ca3	0.35	0.23	0.20	0.15			0.28			0.21				0.34	0.19		1.95
Al			0.47	0.48					0.54+0.48	0.54+0.47							2.98
As1	1.35	1.33	1.20	1.17													5.05
As2					1.30	1.28	1.22	1.21									5.01
H9							0.20		0.80								1.00
H10								0.20		0.80							1.00
H11a						0.19					0.81						1.00
H11b								0.22			0.78						1.00
H12a												0.80		0.20			1.00
H12b												0.83			0.17		1.00
H13a													0.81			0.19	1.00
H13b													0.91			0.09	1.00
H14a					0.21									0.79			1.00
H14b							0.22							0.78			1.00
H15a											0.16				0.84		1.00
H15b															0.88	0.12	1.00
H16a						0.18										0.82	1.00
H16b												0.10				0.90	1.00
Σ_a	1.94	1.91	2.01	1.99	1.93	2.03	1.92	1.93	2.01	2.02	2.07	1.97	2.02	2.11	2.08	2.12	

Multiplicity is indicated by $\times \rightarrow$; bond strengths from Brown and Altermatt (1985); hydrogen-bond strengths based on O···O bond lengths, also from Brown and Altermatt (1985).

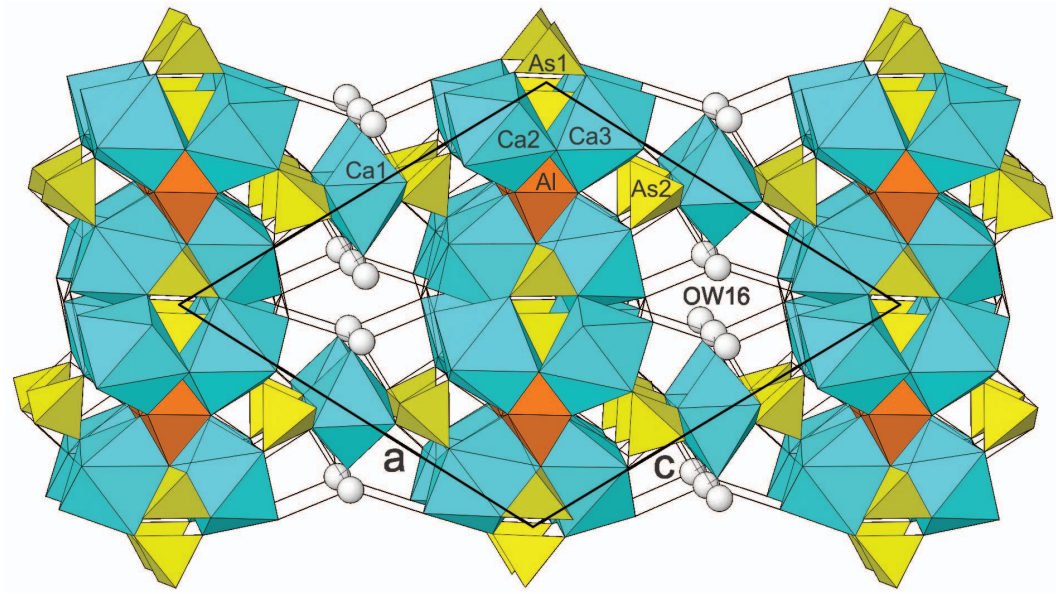

FIG. 3. Structure of tapiaite viewed slightly canted to the *b* axis. Hydrogen bonds are shown as thin black lines. The unit-cell outline is shown as a thick black line.

the columns, sharing two corners with CaO_8 polyhedra. These tetrahedra share their other two corners with CaO_6 octahedra in the interlayer region, thereby linking the layers in the $[10\bar{1}]$ direction and resulting in a framework structure. One isolated H_2O group (OW16) resides in open space in the framework. An extensive system of hydrogen bonds further links the framework.

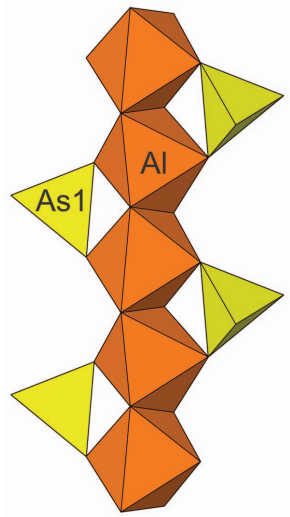

FIG. 4. $Al(AsO_4)(OH)_2$ chain in the structure of tapiaite.

The structure of tapiaite is not closely related to that of any other mineral. The only other mineral containing Ca, Al As, O and H only is arsenocrandallite, $CaAl_3(AsO_4)_2(OH)_5{\cdot}H_2O$, but it has the alunite/jarosite structure type (e.g. Blount, 1974; Mills *et al*., 2013) and exhibits no similarity to that of tapiaite. Joteite, which is closely associated with tapiaite, has a quite dissimilar structure. In the Strunz system, tapiaite fits in subdivision 8.DC: phosphates, arsenates, vanadates with additional anions, with H_2O, with large and medium-sized cations and with (OH, etc.):RO_4 = 1:1 (R = P, As, V).

Acknowledgements

Fernando Cámara, Frank Hawthorne and an anonymous reviewer are thanked for their constructive comments on the manuscript. A portion of this study was funded by the John Jago Trelawney Endowment to the Mineral Sciences Department of the Natural History Museum of Los Angeles County.

References

Blount, A.M. (1974) The crystal structure of crandallite. *American Mineralogist*, **59**, 41–47.

Brown, I.D. and Altermatt, D. (1985) Bond-valence

parameters from a systematic analysis of the inorganic crystal structure database. *Acta Crystallographica*, **B41**, 244–247.

Chopin, C., Brunet, F., Gebert, W., Medenbach, O. and Tillmanns, E. (1993) Bearthite, $Ca_2Al[PO_4]_2(OH)$, a new mineral from high-pressure terranes of the western Alps. *Schweizerische Mineralogische und Petrographische Mitteilungen*, **73**, 1–9.

Fanfani, L. and Zanazzi, P.F. (1968) The crystal structure of vauquelinite and the relationships to fornacite. *Zeitschrift für Kristallographie*, **126**, 433–443.

Higashi, T. (2001) *ABSCOR*. Rigaku Corporation, Tokyo.

Huminicki, D.M.C. and Hawthorne, F.C. (2002) The crystal chemistry of the phosphate minerals. Pp. 123–253 in: *Phosphates* (M.L. Kohn, J. Rakovan and J.M. Hughes, editors). Reviews in Mineralogy & Geochemistry, **48**. Mineralogical Society of America and the Geochemical Society, Chantilly, Virginia, USA.

Kampf, A.R. and Moore, P.B. (1977) Melonjosephite, calcium iron hydroxy phosphate: its crystal structure. *American Mineralogist*, **62**, 60–66.

Kampf, A.R., Mills, S.J., Housley, R.M., Rossman, G.R., Nash, B.P., Dini, M. and Jenkins, R.A. (2013) Joteite, $Ca_2CuAl[AsO_4][AsO_3(OH)]_2(OH)_2(H_2O)_5$, a new arsenate with a sheet structure and unconnected acid arsenate groups. *Mineralogical Magazine*, **77**, 2811–2823.

Kampf, A.R., Mills, S.J., Nash, B., Dini, M. and Molina Donoso, A.A. (2014) Tapiaite, IMA 2014-024. CNMNC Newsletter No. 21, August 2014, page 800; *Mineralogical Magazine*, **78**, 797–804.

Mandarino, J.A. (2007) The Gladstone–Dale compatibility of minerals and its use in selecting mineral species for further study. *The Canadian Mineralogist*, **45**, 307–1324.

Mills, S.J., Birch, W.D., Kampf, A.R., Christy, A.G., Pluth, J.J., Pring, A., Raudsepp, M. and Chen, Y.-S. (2010) Kapundaite, $(Na,Ca)_2Fe_4^{3+}(PO_4)_4(OH)_3{\cdot}5H_2O$, a new phosphate species from Toms quarry, South Australia: description and structural relationship to mélonjosephite. *American Mineralogist*, **95**, 754–760.

Mills, S.J., Nestola, F., Kahlenberg, V., Christy, A.G., Hejny, C. and Redhammer, G.J. (2013) Looking for jarosite on Mars: The low-temperature crystal structure of jarosite. *American Mineralogist*, **98**, 1966–1971.

Parker, R.L., Salas, R.O. and Perez, G.R. (1963) Geologia de los distritos mineros Checo de Cobre Pampa Larga y Cabeza de Vaca. *Instituto de Investigaciones Geologicas*, **14**, 40–42.

Pouchou, J.-L. and Pichoir, F. (1991) Quantitative analysis of homogeneous or stratified microvolumes applying the model "PAP". Pp. 3l–75 in: *Electron Probe Quantitation* (K.F.J. Heinrich and D.E. Newbury, editors). Plenum Press, New York.

Schofield, P.F., Wilson, C.C., Knight, K.S. and Kirk, C.A. (2009) Proton location and hydrogen bonding in the hydrous lead copper sulfates linarite, $PbCu(SO_4)(OH)_2$, and caledonite, $Pb_5Cu_2(SO_4)_3CO_3(OH)_6$. *The Canadian Mineralogist*, **47**, 649–662.

Sheldrick, G.M. (2008) A short history of *SHELX*. *Acta Crystallographica*, **A64**, 112–122.

Yang, H., Jenkins, R.A., Downs, R.T., Evans, S.H. and Tait, K.T. (2011) Rruffite, $Ca_2Cu(AsO_4)_2{\cdot}2H_2O$,a new member of the roselite group, from Tierra Amarilla, Chile. *The Canadian Mineralogist*, **49**, 877–884.